

**Synthesis of the cationic complexes $[(C_5H_4CPh_2)_2Ru]^{2+}$
and $[Ph_2(O)CC_5H_4RuC_5H_4CPh_2]^+$.
Molecular and crystal structures of
 $[Ph_2(O)CC_5H_4RuC_5H_4CPh_2]^+[CF_3SO_3]^- \cdot CHCl_3$ and
 $[C_5H_5RuC_5H_4CPh_2]^+PF_6^-$**

F. M. Dolgushin, A. I. Yanovsky, Yu. T. Struchkov, M. I. Rybinskaya, A. Z. Kreindlin,
P. V. Petrovskii, L. M. Epstein, E. S. Shubina, and A. N. Krylov*

*A. N. Nesmeyanov Institute of Organoelement Compounds, Russian Academy of Sciences,
28 ul. Vavilova, 117813 Moscow, Russian Federation.
Fax: +7 (095) 135 5085*

The formation of the previously unknown $[(C_5H_4CPh_2)_2Ru]^{2+}$ dication was established by 1H and ^{13}C NMR spectroscopy. This cation readily hydrolyzes to form the monocation, $[Ph_2(O)CC_5H_4RuC_5H_4CPh_2]^+$. The latter was characterized by NMR spectroscopy and X-ray structural analysis. For comparison, $[C_5H_5RuC_5H_4CPh_2]^+PF_6^-$ was also studied by X-ray structural analysis. The increase in the M—C $_{\alpha}$ distance and the decrease in the angle of inclination of the CPh $_2$ group to the metal atom in disubstituted ruthenocene compared to those in monosubstituted ruthenocene is related to the presence of a bulky substituent in the second Cp ligand and is likely due to the crystal packing effect. IR spectra and X-ray structural analysis attest to the existence of the OH \cdots OSO $_2$ CF $_3$ hydrogen bond in crystals of the trifluoromethanesulfonate monocation.

Key words: α -metallocenylcarbocation; biscyclopentadienyl ruthenium complexes; IR spectra; NMR spectra; X-ray diffraction study.

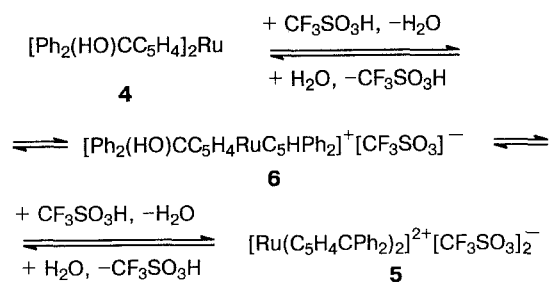
Since the detection of the stability of α -ferrocenyl cations over 30 years ago these systems have drawn the attention of organometallic chemists, who intensely study the structure, chemical behavior, and, mainly, the role of the central transition-metal atom in the stabilization of carbocation centers.^{1,2} Currently, the range of objects under study continues to grow, and in particular, metallocenyl carbocations with different transition-metal atoms and with different substituents on the organic ligands are being studied in detail. Following the study of monocations,^{3,4} we examined⁵ dications prepared from metallocenes of the iron subgroup.* We obtained⁵ the homoannular primary dications $C_5Me_5MC_5Me_3(CH_2^+)_2$, which are formed from the corresponding diols $C_5Me_5MC_5Me_3(CH_2OH)_2$ under the action of CF_3SO_3H . The presumed structures of the salts of these dications were confirmed by 1H and ^{13}C NMR spectroscopy; however, we failed to isolate these salts from a solution in the solid state. Previously, the heteroannular dication $[Ru(C_5H_4CHPh)_2]^{2+}$ was prepared and characterized by 1H NMR spectroscopy.⁷ We

assumed that in the case of heteroannular tertiary dications containing substituents able to additionally stabilize the positive charge, we would succeed not only in generating the dications in solutions, but, probably, in isolating them in the form of the stable salts. For this purpose, we obtained the dication $[(C_5H_4CPh_2)_2Ru]^{2+}$ and studied it by NMR. However, the extremely high susceptibility of this dication to hydrolysis made it possible to isolate only the monocation salt, $[Ph_2(O)CC_5H_4RuC_5H_4CPh_2]^+[CF_3SO_3]^-$, which was studied by X-ray structural analysis.

Results and Discussion

Benzoylation of ruthenocene (**1**) was carried out as reported previously⁸ to give mono- (**2**) and dibenzoylruthenocene (**3**). Reaction of **3** with phenyllithium affords diol $[Ph_2(OH)CC_5H_4]_2Ru$ (**4**). The reaction of **4** with CF_3SO_3H in $CH_3NO_2-CH_2Cl_2$ (or $CD_3NO_2-CD_2Cl_2$) produces a green solution of dication salt **5**, which is confirmed by the 1H and ^{13}C NMR spectra (see Experimental). The addition of absolute toluene or chloroform to this solution results in precipitation of a green oily product; we failed to obtain crystals from this product.

* The detection of ferrocenyl tertiary dications by NMR spectroscopy was first reported in Ref. 6.



Dication **5** hydrolyzes extremely readily. Thus, when even absolute ether was added to the reaction mixture, an orange solution formed; after cooling this solution yielded orange needle-like crystals of the salt $[\text{Ph}_2(\text{HO})\text{CC}_5\text{H}_4\text{RuC}_5\text{HPh}_2]^+[\text{CF}_3\text{SO}_3]^-$ (**6**), which is attributable to partial reversibility of the reaction in the presence of ether, which lowers the acidity of the medium. The elemental analysis data, ^1H and ^{13}C NMR spectral data, and IR absorption spectra confirm the composition and structure of **6**. Crystallization from chloroform afforded a single crystal of the solvate $\mathbf{6} \cdot \text{CHCl}_3$; the single crystal was studied by X-ray structural analysis. The structure of **6** is shown in Fig. 1; bond lengths and bond angles are given in Tables 1 and 2.

The geometry of cation **6** points to a substantially weaker interaction between the metal atom and the carbocation center than in the monosubstituted osmium analog $[\text{C}_5\text{H}_5\text{OsC}_5\text{H}_4\text{CPh}_2]^+\text{PF}_6^-$ (**7**).⁹ The Ru—C $_{\alpha}$ dis-

tance in **6** is 2.648(5) Å, which is nearly 0.4 Å larger than that found in **8** (2.270(3) Å); in **6**, the angle of the deviation of the C $_{\text{Cp}}$ —C $_{\alpha}$ bond from the Cp-ligand plane toward the metal atom (hereinafter, this angle is denoted α) is 27.0° (in **7**, 38.4°). This is quite unexpected because in two derivatives of permethylated metallocenes $[\text{C}_5\text{Me}_5\text{MC}_5\text{Me}_4\text{CH}_2]^+\text{BPh}_4^-$, where M = Ru (**8**)⁴ and Os (**9**),¹⁰ that we have studied, the difference between the ruthenium and osmium complexes with regard to the M—C $_{\alpha}$ distance and the α angle are much less significant (for convenience of comparison, the principal geometric parameters for the structurally studied metallocenyl carbocation complexes of Fe, Ru, and Os are summarized in Table 3; the notations for the parameters are shown in Fig. 2). We suggested that the substantially larger Ru—C $_{\alpha}$ distance in **6** compared to the known values for the Ru and Os derivatives is, apparently, caused by the presence of the bulky substituent in the second Cp ligand and is a result of crystal packing. For this reason we performed X-ray structural analysis of the ruthenium derivative $[\text{C}_5\text{H}_5\text{RuC}_5\text{H}_4\text{CPh}_2]^+\text{PF}_6^-$ (**10**), which we had obtained earlier,^{10,11} for comparison with the analogous Os complex, which been studied previously. The structure of cation **10** is shown in Fig. 3. Bond lengths and bond angles are given in Tables 4 and 5.

It can be seen from Table 3 that the strongest M—C $_{\alpha}$ interaction is observed in complexes **8** and **9**. Apparently, there are two reasons for this phenomenon.

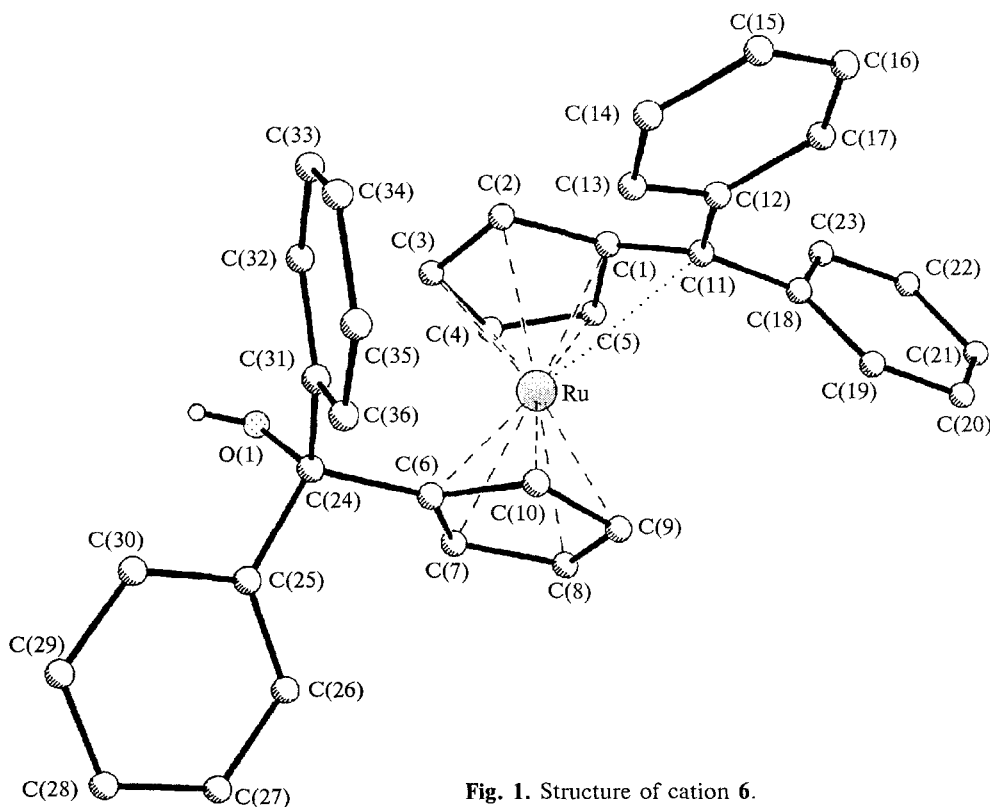


Fig. 1. Structure of cation **6**.

Table 1. Bond lengths in compound **6**

Bond	<i>d</i> /Å	Bond	<i>d</i> /Å	Bond	<i>d</i> /Å
Ru—C(1)	2.120(4)	C(8)—C(9)	1.402(6)	C(26)—C(27)	1.394(6)
Ru—C(2)	2.183(5)	C(9)—C(10)	1.431(7)	C(27)—C(28)	1.365(8)
Ru—C(3)	2.233(6)	C(11)—C(12)	1.489(6)	C(28)—C(29)	1.393(8)
Ru—C(4)	2.202(5)	C(11)—C(18)	1.493(7)	C(29)—C(30)	1.380(6)
Ru—C(5)	2.167(5)	C(12)—C(13)	1.400(7)	C(31)—C(32)	1.391(7)
Ru—C(6)	2.190(4)	C(12)—C(17)	1.406(5)	C(31)—C(36)	1.393(7)
Ru—C(7)	2.159(3)	C(13)—C(14)	1.369(6)	C(32)—C(33)	1.385(6)
Ru—C(8)	2.202(5)	C(14)—C(15)	1.387(5)	C(33)—C(34)	1.362(8)
Ru—C(9)	2.190(6)	C(15)—C(16)	1.373(8)	C(34)—C(35)	1.387(8)
Ru—C(10)	2.176(5)	C(16)—C(17)	1.377(6)	C(35)—C(36)	1.389(6)
O(1)—C(24)	1.430(6)	C(18)—C(19)	1.391(8)	S—O(2)	1.399(4)
C(1)—C(2)	1.452(7)	C(18)—C(23)	1.387(7)	S—O(3)	1.439(5)
C(1)—C(5)	1.459(6)	C(19)—C(20)	1.380(8)	S—O(4)	1.426(5)
C(1)—C(11)	1.420(6)	C(20)—C(21)	1.384(8)	S—C(37)	1.803(5)
C(2)—C(3)	1.413(5)	C(21)—C(22)	1.362(9)	C(37)—F(1)	1.303(9)
C(3)—C(4)	1.406(8)	C(22)—C(23)	1.386(8)	C(37)—F(2)	1.312(9)
C(4)—C(5)	1.390(6)	C(24)—C(25)	1.542(5)	C(37)—F(3)	1.313(6)
C(6)—C(7)	1.427(6)	C(24)—C(31)	1.522(5)	C(38)—Cl(1)	1.740(6)
C(6)—C(10)	1.417(6)	C(25)—C(26)	1.382(7)	C(8)—Cl(2)	1.747(4)
C(6)—C(24)	1.529(7)	C(25)—C(30)	1.408(7)	C(38)—Cl(3)	1.758(5)
C(7)—C(8)	1.423(7)				

Table 2. Principal bond angles in compound **6**

Angle	φ /deg						
C(2)C(1)C(5)	106.6(3)	C(6)C(24)C(25)	110.3(4)	C(11)C(18)C(19)	121.2(4)	C(34)C(35)C(36)	119.7(5)
C(2)C(1)C(11)	124.2(4)	O(1)C(24)C(31)	111.9(4)	C(11)C(18)C(23)	120.1(5)	C(31)C(36)C(35)	120.7(5)
C(5)C(1)C(11)	120.8(5)	C(6)C(24)C(31)	110.0(3)	C(19)C(18)C(23)	118.7(5)	O(2)SO(3)	116.8(3)
C(1)C(2)C(3)	107.6(4)	C(25)C(24)C(31)	110.9(4)	C(18)C(19)C(20)	120.8(5)	O(2)SO(4)	116.9(3)
C(2)C(3)C(4)	108.1(4)	C(24)C(25)C(26)	124.0(4)	C(19)C(20)C(21)	119.5(5)	O(3)SO(4)	111.3(3)
C(3)C(4)C(5)	110.5(4)	C(24)C(25)C(30)	117.7(4)	C(20)C(21)C(22)	120.4(6)	O(2)SC(37)	104.4(3)
C(1)C(5)C(4)	107.1(4)	C(26)C(25)C(30)	118.2(4)	C(21)C(22)C(23)	120.3(5)	O(3)SC(37)	102.7(3)
C(1)C(11)C(12)	123.8(4)	C(25)C(26)C(27)	120.6(5)	C(18)C(23)C(22)	120.3(5)	O(4)SC(37)	102.3(3)
C(1)C(11)C(18)	117.6(4)	C(26)C(27)C(28)	121.2(5)	C(6)C(7)C(8)	108.8(4)	SC(37)F(1)	112.0(4)
C(12)C(11)C(18)	116.6(4)	C(27)C(28)C(29)	118.8(4)	C(7)C(8)C(9)	107.4(4)	SC(37)F(2)	110.4(4)
C(11)C(12)C(13)	125.0(3)	C(28)C(29)C(30)	120.8(5)	C(8)C(9)C(10)	108.8(4)	SC(37)F(3)	112.7(4)
C(11)C(12)C(17)	117.7(4)	C(25)C(30)C(29)	120.4(5)	C(6)C(10)C(9)	107.8(4)	F(1)C(37)F(2)	108.0(6)
C(13)C(12)C(17)	117.2(4)	C(24)C(31)C(32)	121.4(4)	C(7)C(6)C(10)	107.1(4)	F(1)C(37)F(3)	105.1(5)
C(12)C(13)C(14)	121.3(3)	C(24)C(31)C(36)	120.3(4)	C(7)C(6)C(24)	125.9(3)	F(2)C(37)F(3)	108.3(5)
C(13)C(14)C(15)	120.7(5)	C(32)C(31)C(36)	118.2(4)	C(10)C(6)C(24)	126.9(4)	Cl(1)C(38)Cl(2)	110.8(3)
C(14)C(15)C(16)	118.8(4)	C(31)C(32)C(33)	120.9(5)	O(1)C(24)C(6)	105.3(4)	Cl(1)C(38)Cl(3)	109.2(3)
C(15)C(16)C(17)	121.2(4)	C(32)C(33)C(34)	120.3(5)	O(1)C(24)C(25)	108.3(3)	Cl(2)C(38)Cl(3)	109.8(3)
C(12)C(17)C(16)	120.7(4)	C(33)C(34)C(35)	120.2(4)				

Table 3. Selected geometric parameters and the ^{13}C NMR spectrum for carbocations stabilized with π -cyclopentadienyl ligands

Compound	$R(\text{M}-\text{C}_\alpha)/\text{\AA}$	α/deg	β/deg	$\Delta x/\text{\AA}$	$d/\text{\AA}$	$h/\text{\AA}$	δ^*	References
$[\text{C}_5\text{H}_5\text{FeC}_5\text{H}_4\text{CPh}_2]^+[\text{PF}_6]^-$ (11)	2.715	20.7	9.3	0.08	0.50	0.08	171.6	13
$[\text{C}_5\text{H}_5\text{RuC}_5\text{H}_4\text{CPh}_2]^+[\text{PF}_6]^-$ (10)	2.482	34.0	11.3	0.13	0.81	0.15	139.6	**
$[\text{C}_5\text{H}_5\text{OsC}_5\text{H}_4\text{CPh}_2]^+[\text{PF}_6]^-$ (7)	2.387	38.4	14.1	0.46	0.91	0.23	95.7	8
$[\text{C}_5\text{Me}_5\text{RuC}_5\text{Me}_4\text{CH}_2]^+[\text{BPh}_4]^-$ (8)	2.270	40.3	6.8	0.20	0.92	0.09	74.6	4
$[\text{C}_5\text{Me}_5\text{OsC}_5\text{Me}_4\text{CH}_2]^+[\text{BPh}_4]^-$ (9)	2.224	42.5	6.9	0.20	0.98	0.12	55.4	9
$[\text{Ph}_2(\text{HO})\text{CC}_5\text{H}_4\text{RuC}_5\text{H}_4\text{CPh}_2]^+[\text{CF}_3\text{SO}_3]^-$ (6)	2.648	27.0	11.6	0.10	0.65	0.12	139.3	**

* See Refs. 3 and 8.

** Results of this work.

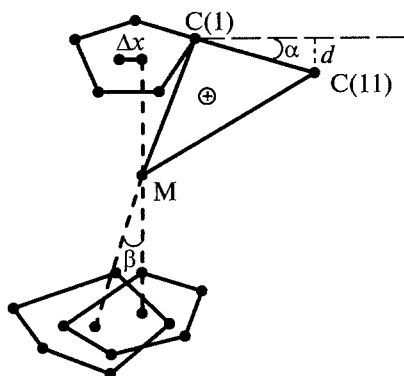


Fig. 2. Geometric parameters of metallocenylmethyl cations.

On the one hand, the methyl substituents in the Cp ligands exhibit electron-donor properties (compared to the hydrogen atoms in the other complexes) resulting in an increase in electron density on the metal atom and enhancing its capability for stabilizing the exocyclic

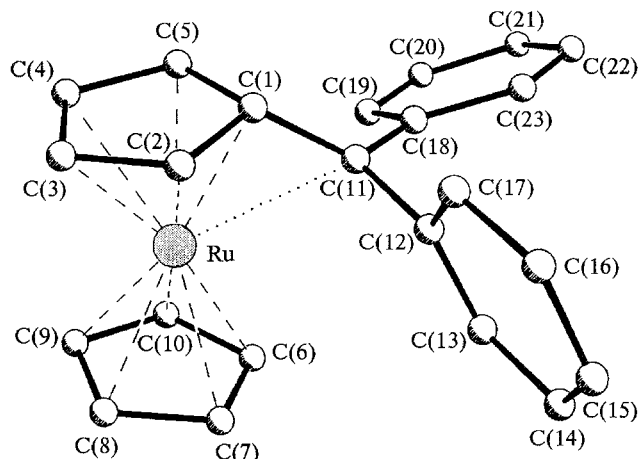


Fig. 3. Structure of cation 10.

carbocation center. On the other hand, it is known that strengthening of the $M-C_{\alpha}$ interaction is favored by the

Table 4. Bond lengths in compound 10

Bond	$d/\text{\AA}$	Bond	$d/\text{\AA}$	Bond	$d/\text{\AA}$
Ru—C(1)	2.098(2)	C(6)—C(7)	1.427(3)	C(19)—C(20)	1.392(2)
Ru—C(2)	2.167(2)	C(6)—C(10)	1.414(3)	C(20)—C(21)	1.388(3)
Ru—C(3)	2.222(2)	C(7)—C(8)	1.421(3)	C(21)—C(22)	1.386(3)
Ru—C(4)	2.232(2)	C(8)—C(9)	1.439(4)	C(22)—C(23)	1.386(2)
Ru—C(5)	2.182(2)	C(9)—C(10)	1.420(3)	P—F(1)	1.59(1)
Ru—C(6)	2.199(2)	C(11)—C(12)	1.489(2)	P—F(2)	1.58(1)
Ru—C(7)	2.184(3)	C(11)—C(18)	1.497(2)	P—F(3)	1.546(6)
Ru—C(8)	2.174(3)	C(12)—C(11)	1.489(2)	P—F(4)	1.616(5)
Ru—C(9)	2.173(3)	C(12)—C(13)	1.396(3)	P—F(5)	1.570(8)
Ru—C(10)	2.213(3)	C(12)—C(17)	1.394(3)	P—F(6)	1.599(8)
Ru—C(11)	2.482(2)	C(13)—C(14)	1.386(2)	P—F(1')	1.60(2)
C(1)—C(2)	1.458(2)	C(14)—C(15)	1.388(3)	P—F(2')	1.64(2)
C(1)—C(5)	1.463(3)	C(15)—C(16)	1.386(3)	P—F(3')	1.62(1)
C(1)—C(11)	1.421(2)	C(16)—C(17)	1.394(3)	P—F(4')	1.54(1)
C(2)—C(3)	1.413(3)	C(18)—C(11)	1.497(2)	P—F(5')	1.61(1)
C(3)—C(4)	1.421(3)	C(18)—C(19)	1.398(3)	P—F(6')	1.55(2)
C(4)—C(5)	1.414(2)	C(18)—C(23)	1.402(2)		

Table 5. Principal bond angles in compound 10

Angle	φ/deg	Angle	φ/deg	Angle	φ/deg	Angle	φ/deg
C(2)C(1)C(5)	107.2(1)	F(1)PF(2)	178.0(8)	C(11)C(12)C(17)	120.6(2)	F(2')PF(3')	96.1(10)
C(2)C(1)C(11)	119.3(1)	F(1)PF(3)	88.8(4)	C(13)C(12)C(17)	119.4(2)	F(1')PF(4')	90.7(9)
C(5)C(1)C(11)	120.9(1)	F(2)PF(3)	90.3(5)	C(12)C(13)C(14)	120.3(2)	F(2')PF(4')	85.0(10)
C(1)C(2)C(3)	107.3(2)	F(1)PF(4)	90.1(4)	C(13)C(14)C(15)	120.1(2)	F(3')PF(4')	172.3(8)
C(2)C(3)C(4)	109.2(2)	F(1)PF(5)	89.0(7)	C(14)C(15)C(16)	119.8(2)	F(1')PF(5')	92.2(13)
C(3)C(4)C(5)	109.2(2)	F(2)PF(5)	92.8(6)	C(15)C(16)C(17)	120.4(2)	F(2')PF(5')	86.1(10)
C(1)C(5)C(4)	107.1(2)	F(3)PF(5)	94.6(4)	C(12)C(17)C(16)	119.8(2)	F(3')PF(5')	83.8(7)
C(7)C(6)C(10)	109.1(2)	F(4)PF(5)	89.3(3)	C(11)C(18)C(19)	124.8(1)	F(4')PF(5')	88.7(7)
C(6)C(7)C(8)	107.8(2)	F(1)PF(6)	90.0(7)	C(11)C(18)C(23)	116.9(2)	F(1')PF(6')	88.9(13)
C(7)C(8)C(9)	107.2(2)	F(2)PF(6)	88.2(6)	C(19)C(18)C(23)	118.3(1)	F(2')PF(6')	93.2(11)
C(8)C(9)C(10)	108.6(2)	F(3)PF(6)	89.4(4)	C(18)C(19)C(20)	120.4(2)	F(3')PF(6')	90.1(8)
C(6)C(10)C(9)	107.3(2)	F(4)PF(6)	86.7(3)	C(19)C(20)C(21)	120.4(2)	F(4')PF(6')	97.4(8)
C(1)C(11)C(12)	119.1(1)	F(5)PF(6)	175.9(3)	C(20)C(21)C(22)	119.7(2)	F(5')PF(6')	173.8(7)
C(12)C(11)C(18)	114.9(1)	F(1')PF(2')	175.4(14)	C(21)C(22)C(23)	120.1(2)		
C(11)C(12)C(13)	119.9(2)	F(1')PF(3')	87.9(9)	C(18)C(23)C(22)	121.0(2)		

absence of phenyl substituents at the carbocation center; these substituents partially delocalize its positive charge. As an illustration of the latter statement, we can mention the results of the structural investigation of two chromium complexes, $(OC)_3CrC_5H_4CR_2$, where $R = H$ and Ph ; in the former complex, the $M-C_\alpha$ distance (2.352 Å)¹² is substantially smaller than that in the latter complex (2.548 Å).¹³

It should be emphasized that the reasons for these substantial changes in the geometry of complex **6** compared to **10** (see Table 3) are not totally clear. Apparently, even insignificant energy effects, such as the crystal field effect, can substantially affect the $M-C_\alpha$ distance.

The structure of **10** is the missing element in the series of compounds $[C_5H_5MC_5H_4CPh_2]^+PF_6^-$, where $M = Fe$,¹⁴ Ru , and Os ⁹ (see Table 3).

The geometry of these cations confirms the existing concept that the stability of the carbocations in complexes of Group VIII transition metals increases as the atomic number increases.^{1,2,9} As expected, the change in geometry is substantially more pronounced on passing from iron to ruthenium than on passing from ruthenium to osmium.

The common structural feature of all of the studied α -metallocenyl carbocations is the asymmetric position of the metal atom with respect to the substituted Cp ring, which manifests itself in the shift of the metal atom toward the exocyclic C_α atom (parameter Δx in Table 3 can be defined as the distance between the projection of the metal atom to the plane of the Cp ring and the center of this ring). The shift of the metal atom toward the C(1)—C(11) bond and the deviation of the C_α atom from the plane of the Cp ring (parameter d in Table 3) toward the metal atom correlate with the significant redistribution of the $M-C_{Cp}$ distances and the C—C bond lengths in the ligand containing the carbocationic center in complexes **6** and **10**. Thus, the $Ru-C(1)$ distance is substantially shorter (2.120(4) Å in **6** and 2.098(2) Å in **10**); the $Ru-C(2)$ and $Ru-C(5)$ distances are virtually the same (2.183(5) and 2.167(5) Å in **6**, 2.167(2) and 2.182(2) Å in **10**); whereas the $Ru-C(3)$ and $Ru-C(4)$ distances are slightly longer (2.233(6) and 2.202(5) Å in **6**, 2.222(2) and 2.232(2) Å in **10**) than the mean bond length between the Ru atom and the carbon atoms that are not linked with the carbocationic center of the ring (2.183 Å in **6** and 2.189 Å in **10**). The distribution of the C(1)—C(5) bond lengths in the cycle in **6** is in good agreement with those observed previously in all of the carbocationic complexes in which $M-C_\alpha$ interaction exists: the C(1)—C(2) and C(1)—C(5) bonds are, on the average, 0.05 Å longer than the remaining three bonds C(2)—C(3), C(3)—C(4), and C(4)—C(5) in the cycle (see Tables 2 and 5).

The exocyclic C(1)—C(11) bond (1.420(6) Å in **6** and 1.421(2) Å in **10**) is substantially shorter than the exocyclic C—C single bond in metallocenes.

This may be caused by a strong donor—acceptor interaction between the metal atom and the carbocationic center and by the formation of a three-membered metal-cycle in which the metal atom has a high positive charge. As is known, the positive charge is effectively stabilized in cyclopropenyl cation. Apparently, the shortening of the $C_{Cp}-C_\alpha$ bond is caused by the formation of a stable ion, something like metallocyclopropenyl cation, which is favored by the system of conjugated bonds of the cyclopentadienyl ring. The metal atom in these ions (this is particularly true for ion **9**) is an onium atom, and hence we called these particles metallonium or metalloconium compounds, as a special case of metallocenyl compounds. As we have already demonstrated,¹⁵ the major part of the positive charge in monocations of the type $[C_5R_5MC_5R_4CH_2]^+$ ($M = Ru$ and Os ; $R = H$ and Me) is localized on the metal atom. According to the results that we obtained earlier^{4,9,10} and the results of the present work, the absence of Me substituents in the Cp ring and the presence of Ph substituents at the exocyclic carbon atom have little effect on the geometry of the molecule. From the preliminary assessment, it can be assumed that molecules of this type also have similar electronic structures and similar charge distributions. It is for this reason that we want to call attention to the possibility of the occurrence of a "cyclopropenyl cation" (see Fig. 2). In our opinion, this allows one to interpret the cause of the shortening of the C(1)—C(11) bond in a different way.

Like in the studied^{4,9,10,12–14,16,17} complexes of Fe, Cr, Mo, W, Os, and Ru, no substantial distortion of planarity was found in the Cp ligand linked to the carbocation center in cations **6** and **10**. Though the C(1) atom is displaced from the C(2)C(3)C(4)C(5) plane toward the Ru atom, this deviation is no more than 0.02 and 0.04 Å in **6** and **10**, respectively; the dihedral angle between this plane and the plane through C(2)C(1)C(5) is very small: 1.6 and 2.4°, respectively.

The Cp rings C(1)—C(5) and C(6)—C(10) are not coplanar; the angles between these planes are 11.6° (**6**) and 11.3° (**10**) (angle β in Table 3). This effect is observed in all metallocenyl carbocationic complexes and it can be associated with the $M-C_\alpha$ interaction. However, there is no strict correlation, because for the substantially stronger $M-C_\alpha$ interaction in complexes **8** and **9**, the dihedral angles between the planes of the Cp rings are essentially smaller and equal 6.8 and 6.9°, respectively. However, it is obvious that the value of this dihedral angle cannot be independent of the degree of substitution of the Cp ligand and the carbocation center.

The mutual orientation of the Cp rings in the reported complexes changes over a very wide range. In cation **6**, the C(1)Cp(1)Cp(2)C(7) torsion angle (Cp(1) and Cp(2) are the centers of the Cp rings C(1)—C(5) and C(6)—C(10), respectively) is 166.1°, which corresponds to a conformation intermediate between staggered and eclipsed. It is interesting to note that in the series $[C_5H_5MC_5H_4CPh_2]^+$, where $M = Fe$, Ru , and

Os, the torsion angles are 153, 160, and 161°, respectively; that is, in the iron complex, the conformation is nearly eclipsed, whereas in the Ru and Os analogs, intermediate conformations are realized. In complexes **8** and **9**, which contain methylated Cp ligands, the similar torsion angle is 178°, that is, in these complexes the staggered conformation of the Cp rings is realized.

In the crystal of **6**, an O—H...O hydrogen bond is present, which involves the OH group of the cation and one of the oxygen atoms of the CF₃SO₃⁻ anion (O(1)—H(1) 0.7(1), O(1)...O(4) 2.744(6), and H(1)...O(4) 2.0(1) Å; the O(1)H(1)O(4) angle is 162(7)°. In addition, the contact between the solvate chloroform molecule and the anion, namely, the C(38)...O(3) distance, 3.04(5) Å, is shortened (the sum of van der Waals radii for C and O is 1.7 + 1.5 = 3.2 Å, *cf.* Ref. 18). Apparently, this is caused by the formation of a C—H...O hydrogen bond and is attributable to the increased acidity of the hydrogen atom in the chloroform molecule. The extensive statistical data on C—H...Y hydrogen bonds, where Y = O, N, Cl, and S, is generalized with the use of the Cambridge Structural Database.¹⁹ The O(3)...H(38) distance in **6** is 2.23 Å and falls within the range reported previously,¹⁹ though this distance is in the region of weak interactions. The C(38)—H(38)...O(3) angle (141°) also corresponds to the literature data,¹⁹ according to which the mean angle at the hydrogen atom for C—H...O hydrogen bonds is, on the average, smaller than that observed for O—H...O hydrogen bonds. The formation of H-bonds results in an appreciable difference in the S—O bond lengths in the CF₃SO₃⁻ anion: the S—O(2) bond (1.399(4) Å), the O(2) atom of which does not participate in the H-bond, is substantially shorter than the two other S—O bonds (S—O(3) 1.439(5) and S—O(4) 1.426 Å), whose O atoms are involved in hydrogen bonds.

Because a hydrogen bond with the anion was found in crystal **6**, it was of interest to examine the possibility of a change in its character in solution. For this purpose, salt **6**, diol **4**, and [Ph₂(HO)CC₅H₄RuC₅H₄CPh₂]⁺BF₄⁻ (**12**) were studied by IR spectroscopy in the solid state (in the form of suspensions in vaseline oil) and as solutions in CH₂Cl₂.

In the IR spectra of solid samples of **6** and **12**, broad stretching bands for bonded OH groups are observed (3400—3500 cm⁻¹). In the IR spectra of dilute solutions (C = 2 · 10⁻³ M in CH₂Cl₂), the bands for free hydroxyl groups at 3600 cm⁻¹ are observed, which is indicative of the cleavage of intermolecular H-bonds.

The position of the absorption band of the bonded OH groups depends on the counter-ion. The ν(OH) frequencies are 3490 and 3400 cm⁻¹ for salt **12** and compound **6**, respectively. As expected, stronger H-bonds are formed with the CF₃SO₃⁻ anions, which is in agreement with the X-ray structural data for compound **6**.

The spectrum of the original diol **4** does not change in the transition from a solid sample to a dilute solution.

In the ν(OH) region, two bands at 3600 and 3450 cm⁻¹ are observed, which correspond to free OH groups and to the OH groups bonded to the metal atom through the intramolecular H-bond.^{20,21}

Experimental

¹H and ¹³C NMR spectra were recorded on a Bruker WP-200-SY instrument operating at 200.13 and 50.31 MHz. The synthesis of C₅H₅RuC₅H₄C(OH)Ph₂ and [C₅H₅RuC₅H₄CPh₂]⁺PF₆⁻ from **2** has been described previously.^{9,11}

[C₅H₄C(OH)Ph₂]₂Ru (**4**). A 1.2 M solution of PhLi (3.5 mL) was added dropwise with stirring under an Ar atmosphere to a solution of (C₅H₄COPh)₂Ru⁸ (0.44 g, 1 mmol) in absolute ether (200 mL). After 1 h, the reaction mixture was poured into a saturated aqueous solution of NH₄Cl and extracted with ether. The organic layer was dried with Na₂SO₄ and evaporated. Crystallization from a hexane—benzene mixture afforded 0.38 g (63 %) of compound **4**, m.p. 188—189 °C. Found (%): C, 72.46; H, 4.97. C₃₆H₃₀O₂Ru. Calculated (%): C, 72.59; H, 5.08. ¹H NMR (CDCl₃, δ): 3.04 (s, 2 H, OH); 4.50 (s, 8 H, C₅H₄); 7.24 (s, 20 H, Ph).

[Ph₂(HO)CC₅H₄RuC₅H₄CPh₂]⁺[CF₃SO₃]⁻ (**6**). Diol **4** (0.2 g, 0.34 mmol) was dissolved in 5 mL of a 1 : 1 CH₂Cl₂—CH₃NO₂ mixture; then 0.5 mL of CF₃SO₃H was added to the solution. The color of the solution changed from pale-yellow to emerald-green, which is indicative of the formation of cation **5**. ¹H NMR (CF₃SO₃H—CF₃COOH—CD₂Cl₂, δ, J/Hz): 5.87 (t, 2 H, α-H, C₅H₄, J = 2); 6.48 (t, 2 H, β-H, C₅H₄, J = 2); 7.52 (d, 8 H, o-H, Ph, J = 7.2); 7.59 (t, 8 H, m-H, Ph, J = 7.2); 8.12 (t, 4 H, p-H, Ph, J = 7.2). ¹³C NMR (CH₃NO₂—CF₃SO₃H, δ): 89.53 (C(2,5), C₅H₄); 91.84 (C(3,4), C₅H₄); 97.02 (C(1), C₅H₄); 130.50 (m-C, Ph); 136.45 (o-C, Ph); 139.74 (p-C, Ph); 139.78 (C(1), Ph); 201.3 (C⁺).

The reaction mixture was poured into 100 mL of absolute ether, which resulted in a bright-orange solution. Cooling of this solution overnight at -10 to -15 °C yielded orange needle-like crystals of **6** (0.22 g, 90 %), m.p. 156—158 °C (decomp.). Found (%): C, 60.81; H, 4.32; F, 8.57; S, 4.23. C₃₇H₂₉F₃O₄RuS. Calculated (%): C, 61.07; H, 4.02; F, 7.83; S, 4.41. ¹H NMR* (CDCl₃, δ): 4.95 (s, 2 H, C₅H₄); 5.24 (s, 2 H, C₅H₄); 5.29 (s, 2 H, C₅H₄); 6.30 (s, 2 H, C₅H₄); 7.10—7.53 (m, 20 H, Ph). ¹³C NMR (CH₂Cl₂, δ): 76.52, 82.53, 83.73, 87.77, 93.68 (C—C₅H₄); 101.39 (C—OH); 117.41, 126.82, 128.21, 128.88, 131.21, (C—CF₃, C—Ph); 139.3 (C⁺); 144.69, 145.86 (C(1), Ph).

The ¹H and ¹³C NMR spectra of C₅H₅RuC₅H₄C(OH)Ph₂ and cation **10** were reported in Refs. 9 and 11.

Synthesis of [Ph₂(HO)CC₅H₄RuC₅H₄CPh₂]⁺BF₄⁻ (**12**). A solution (0.5 mL) of HBF₄/CF₃COOH (prepared by dissolving 48 % aqueous HBF₄ in (CF₃CO)₂O) was added to a solution of diol **4** (0.2 g, 0.34 mmol) in 5 mL of CH₂Cl₂. The color of the solution changed from pale-yellow to emerald-green. The addition of this mixture to 100 mL of absolute ether afforded an orange precipitate. This precipitate was filtered off and washed with ether to give ~0.2 g (94 %) of **12**. ¹H NMR* (CD₂Cl₂, δ): 4.97 (t, 2 H, C₅H₄); 5.28 (m,

* Proton resonance signals for compounds **6** and **12** are broadened singlets, the band width is ~4 Hz.

Table 6. Atomic coordinates ($\times 10^4$) for compound **6**

Atom	<i>x</i>	<i>y</i>	<i>z</i>	Atom	<i>x</i>	<i>y</i>	<i>z</i>
Ru	2107(1)	3588(1)	2686(1)	C(24)	2228(4)	4074(3)	5213(3)
O(1)	3473(3)	3902(3)	5260(2)	C(25)	2417(4)	5065(3)	6270(3)
C(1)	1735(4)	2119(3)	1282(3)	C(26)	2665(4)	6193(4)	6400(3)
C(2)	2050(4)	1826(4)	2172(3)	C(27)	2929(4)	7060(4)	7400(4)
C(3)	3397(4)	2584(4)	2797(3)	C(28)	2962(4)	6824(4)	8275(4)
C(4)	3918(4)	3326(4)	2315(3)	C(29)	2704(4)	5689(4)	8155(3)
C(5)	2957(4)	3062(4)	1389(3)	C(30)	2425(4)	4817(4)	7169(3)
C(6)	2003(4)	4434(3)	4296(3)	C(31)	1038(4)	2972(3)	5002(3)
C(7)	3023(4)	5222(3)	4070(3)	C(32)	1101(5)	1886(4)	4577(3)
C(8)	2388(4)	5424(4)	3226(3)	C(33)	-9(5)	885(4)	4347(3)
C(9)	995(4)	4733(4)	2902(3)	C(34)	1184(5)	950(4)	4538(4)
C(10)	746(4)	4109(4)	3552(3)	C(35)	1280(5)	2019(4)	4962(4)
C(11)	425(4) ‡	2027(3)	802(3)	C(36)	-171(4)	3025(4)	5193(3)
C(12)	-861(4)	1245(3)	855(3)	S	4574(1)	2682(1)	7384(1)
C(13)	-1056(4)	1077(3)	1762(3)	O(2)	3353(4)	1787(4)	7213(3)
C(14)	-2231(4)	265(4)	1722(3)	O(3)	5709(4)	2365(3)	7235(3)
C(15)	-3282(5)	-397(4)	781(4)	O(4)	4492(4)	3483(3)	6939(3)
C(16)	-3120(5)	-230(4)	-113(3)	C(37)	5109(6)	3577(5)	8789(4)
C(17)	-1937(4)	570(4)	-90(3)	F(1)	5283(6)	3002(4)	9351(3)
C(18)	298(4)	2481(4)	-31(3)	F(2)	4198(4)	3992(5)	9051(3)
C(19)	-538(4)	3082(4)	-90(3)	F(3)	6281(3)	4453(3)	9101(2)
C(20)	-682(5)	3466(4)	-883(4)	C(38)	5925(5)	10(4)	6480(3)
C(21)	9(5)	3244(4)	-1631(4)	Cl(1)	5209(2)	-288(2)	7431(1)
C(22)	813(5)	2639(4)	-1594(4)	Cl(2)	5304(2)	-1227(1)	5284(1)
C(23)	965(4)	2254(4)	-798(3)	Cl(3)	7701(1)	501(1)	6951(1)

Table 7. Atomic coordinates ($\times 10^4$) for compound **10**

Atom	<i>x</i>	<i>y</i>	<i>z</i>	Atom	<i>x</i>	<i>y</i>	<i>z</i>
Ru	1952(1)	2892(1)	1859(1)	C(19)	-1073(2)	5533(2)	2784(2)
C(1)	462(2)	3000(2)	891(2)	C(20)	-2017(2)	6697(2)	3216(2)
C(2)	1447(2)	1770(2)	538(2)	C(21)	-3582(2)	6804(2)	3570(2)
C(3)	2965(2)	2005(2)	-172(2)	C(22)	-4208(2)	5743(2)	3504(2)
C(4)	2960(2)	3335(2)	-308(2)	C(23)	-3275(2)	4581(2)	3086(2)
C(5)	1438(2)	3972(2)	316(2)	P	7649(1)	2093(1)	-1645(1)
C(6)	1317(3)	3370(2)	3967(2)	F(1)	8534(16)	2844(8)	-2950(13)
C(7)	1813(3)	2035(2)	3745(2)	F(2)	6747(13)	1324(12)	-380(12)
C(8)	3362(3)	1847(2)	2802(3)	F(3)	8523(7)	835(6)	-2417(7)
C(9)	3801(3)	3082(3)	2444(3)	F(4)	6665(5)	3416(6)	-900(6)
C(10)	2537(3)	4016(2)	3177(2)	F(5)	8901(7)	2255(6)	-1125(6)
C(12)	-1532(2)	2085(1)	2838(2)	F(6)	6322(7)	2033(7)	-2146(6)
C(13)	-1989(2)	1944(2)	4213(2)	F(1')	8761(33)	2655(18)	-3001(26)
C(14)	-2724(2)	936(2)	4847(2)	F(2')	6537(25)	1605(24)	-193(24)
C(15)	-3036(2)	73(2)	4121(2)	F(3')	8133(17)	725(11)	-2412(10)
C(16)	-2626(3)	230(2)	2763(2)	F(4')	7397(14)	3354(10)	-897(13)
C(17)	-1872(2)	1233(2)	2115(2)	F(5')	9042(11)	1587(10)	-1214(11)
C(18)	-1687(2)	4460(1)	2695(2)	F(6')	6326(13)	2430(15)	-2110(14)

2 H, C₅H₄); 5.25 (t, 2 H, C₅H₄); 6.32 (t, 2 H, C₅H₄); 7.1–7.6 (m, 20 H, C₆H₅).

X-ray structural analysis. Crystals of **6** and **10** are triclinic, at -80 °C: *a* = 10.822(5) and 9.680(2), *b* = 13.315(6) and 10.677(2), *c* = 14.019(6) and 10.968(2) Å, α = 109.97(3) and 87.34(2), β = 99.01(3) and 66.00(2), γ = 108.01(3) and 80.72(2)°, *V* = 1726(1) and 1021.8(3) Å³, *d*_{calc} = 1.630 and 1.760 g cm⁻³ for **6** and **10**, respectively, *Z* = 2, space group *P1*. The unit-cell parameters and intensities for 5575 and 8240 independent reflections were measured on a Syntex P2₁ four-circle automated diffractometer (-80 °C, Mo-K α radiation, graphite monochromator, $\theta/2\theta$ -scanning technique, θ \leq 25 and 34°).

In both cases, the structures were solved by the heavy-atom method. Atomic coordinates for Ru were obtained from the Patterson synthesis, the remaining nonhydrogen atoms were located from subsequent electron density syntheses. The OH hydrogen atom in **6** was located from the electron density maps and was refined isotropically; all the remaining H atoms were placed in calculated positions (C–H 0.96 Å) and are included in the final refinement using a riding model with a common refined isotropic temperature factor (*U*_{iso} = 0.039(2) Å²). All hydrogen atoms in **10** were located from the difference Fourier synthesis and were included in the final refinement with isotropic thermal parameters. The final *R* values: *R* = 0.0351 and 0.0328, *R*_w = 0.0417 and 0.0480,

GOF = 1.58 and 1.01 for 4054 and 7110 reflections with $I > 3\sigma(I)$ for compounds **6** and **10**, respectively.

All calculations were carried out using the SHELXTL PLUS (PS Version)²² program on an IBM PC computer. Atomic coordinates are given in Tables 6 and 7.

References

1. A. A. Koridze, *Usp. Khim.*, 1986, **55**, 277 [*Russ. Chem. Rev.*, 1986, **55** (Engl. Transl.)].
2. W. E. Watts, *J. Organomet. Chem. Libr.*, 1979, **7**, 399.
3. M. I. Rybinskaya, A. Z. Kreindlin, and S. S. Fadeeva, *J. Organomet. Chem.*, 1988, **358**, 363.
4. A. I. Yanovsky, Yu. T. Struchkov, A. Z. Kreindlin, and M. I. Rybinskaya, *J. Organomet. Chem.*, 1989, **369**, 125.
5. A. Z. Kreindlin, E. I. Fedin, P. V. Petrovskii, M. I. Rybinskaya, R. M. Minaev, and R. Hoffmann, *Organometallics*, 1991, **10**, 1206.
6. C. U. Pittman, *Tetrahedron Lett.*, 1967, **37**, 3619.
7. M. N. Nefedova, I. A. Mamedyarova, P. V. Petrovskii, and V. I. Sokolov, *J. Organomet. Chem.*, 1992, **425**, 125.
8. M. D. Raush, E. O. Fisher, and H. Grubert, *J. Am. Chem. Soc.*, 1960, **82**, 76.
9. U. Turpeinen, A. Z. Kreindlin, P. V. Petrovskii, and M. I. Rybinskaya, *J. Organomet. Chem.*, 1992, **441**, 109.
10. M. I. Rybinskaya, A. Z. Kreindlin, Yu. T. Struchkov, and A. I. Yanovsky, *J. Organomet. Chem.*, 1989, **359**, 233.
11. A. Z. Kreindlin, L. S. Shilovtseva, P. V. Petrovskii, and M. I. Rybinskaya, *Metalloorg. Khim.*, 1992, **5**, 1047 [*Organomet. Chem. USSR*, 1992, **5** (Engl. Transl.)].
12. B. Lubke, F. Edelman, and U. Behrens, *Chem. Ber.*, 1983, **116**, 11.
13. V. G. Andrianov and Yu. T. Struchkov, *Zh. Strukt. Khim.*, 1977, **18**, 318 [*J. Struct. Chem.*, 1977, **18** (Engl. Transl.)].
14. U. Behrens, *J. Organomet. Chem.*, 1979, **182**, 89.
15. E. G. Gal'pern, N. P. Gambaryan, A. Z. Kreindlin, M. I. Rybinskaya, I. V. Stankevich, and A. L. Chistyakov, *Metalloorg. Khim.*, 1992, **5**, 831 [*Organomet. Chem. USSR*, 1992, **5** (Engl. Transl.)].
16. A. G. Orpen, L. Brammer, F. H. Allen, O. Kennard, D. G. Watson, and R. Taylor, *J. Chem. Soc., Dalton Trans.*, 1989, 1.
17. J. A. Bandy, V. S. B. Mtetwa, K. Prout, J. C. Green, C. E. Davies, M. L. Green, N. I. Hazel, A. Izquierdo, and J. J. Martin-Polo, *J. Chem. Soc., Dalton Trans.*, 1985, 2037.
18. S. S. Batsanov, *Zh. Neorg. Khim.*, 1991, **36**, 3015 [*Russ. J. Inorg. Chem.*, 1991, **36** (Engl. Transl.)].
19. R. Taylor and O. Kennard, *J. Am. Chem. Soc.*, 1982, **104**, 5063.
20. E. S. Shubina, L. M. Epstein, T. B. Timofeeva, Yu. T. Struchkov, A. Z. Kreindlin, S. S. Fadeeva, and M. I. Rybinskaya, *J. Organomet. Chem.*, 1991, **401**, 133.
21. E. S. Shubina, L. M. Epshtein, A. Z. Kreindlin, S. S. Fadeeva, and M. I. Rybinskaya, *J. Organomet. Chem.*, 1991, **401**, 145.
22. W. Robinson and G. M. Sheldrick, *SHELX*, in *Crystallographic Computing-Techniques and New Technologies*, Eds. N. M. Isaacs and M. R. Taylor, Oxford Univ. Press, Oxford, England, 1988, 366.

Received February 25, 1994